Journal of the Korean Physical Society, Vol. 53, No. 5, November 2008, pp. 2840∼2843

Dynamics of Stimulated Emission in Single ZnO Nanorod Resonators

Johannes Fallert,* Felix Stelzl, Huijuan Zhou,
Markus Wissinger, Mario Hauser, Claus Klingshirn and Heinz Kalt
Institut für Angewandte Physik, Universität Karlsruhe, 76131 Karlsruhe, Germany

Dong Sik Kim
Max Planck Institute of Microstructure Physics, 06120 Halle, Germany

Margit Zacharias
*Institut für Mikrosystemtechnik, Faculty of Applied Science,
Albert Ludwigs University Freiburg, 79110 Freiburg, Germany*

Anton Reiser, Klaus Thonke and Rolf Sauer
Institut für Halbleiterphysik, Universität Ulm, 89069 Ulm, Germany

(Received 10 September 2007)

ZnO nanorods grown via vapor transport methods have been studied under high optical excitation. Via a focused ion beam (FIB), particular nanorods have been marked on the substrate for optical measurements on as-grown single rods. In the particular nanorods, stimulated emission occurs above a certain excitation threshold. A time-resolved measurement of the single nanorod emission is accomplished by the use of a streak-camera. We focus on the typical lasing dynamics, which is found in these measurements on several samples. We explain the complex dynamics after pulsed excitation, which is caused by the interplay of gain competition among several lasing modes, the bandgap renormalization, and the carrier-density-dependent refractive index.

PACS numbers: 78.55.Et, 78.45.+h
Keywords: ZnO, Nanorods, Nanowires, Lasing, Stimulated emission

I. INTRODUCTION

Zinc oxide (ZnO) is of significant interest for-light emitting devices in the ultraviolet (UV). In particular, ZnO nanorods offer the possibility for realizing nanoscaled lasers in the UV. In such a nanorod structure, ZnO not only acts as gain medium for stimulated emission, but also as the laser resonator. The lasing emission wavelength is defined by the guided modes of the nanorod, which depend on its geometry.

We report on investigations of stimulated emission of single nanorods and discuss the observed mode pattern, the shift and gain competition of the lasing modes. Here, several types of samples with ZnO nanorods, grown by using vapor phase transport methods, are examined. For the first kind of sample, ZnO nanorods were grown on a GaN/Al_2O_3 substrate. A pattern of gold droplets as a growth catalyst was assembled on the substrate by the use of an ordered layer of polystyrene nanospheres as a mask for the gold deposition. In a second method, gold nanoparticles were dispersed directly on a GaN/Al_2O_3 substrate. In the third kind of sample, ZnO nanorods were grown on an iridium layer deposited on a silicon substrate. The details of this growth technique have been reported in Ref. 1. The motivation of such an iridium metal layer as an interface between the nanorod and the substrate is to achieve good resonator properties for the nanorod. The transmission into the substrate, which is expected to be the main loss factor [2], should be reduced by the metal layer. A common issue in the optical measurements of single nanorods is that the nanorods grow in dense arrays, prohibiting spectroscopy of individual specimens. Therefore it is common to detach the nanorods from the original substrate and then to disperse them in a dilution [3,4]. In this work we present the measurement of the lasing dynamics of individual ZnO nanorods, which are still attached as grown on their original substrate, by using time-resolved μ-photoluminescence.

*E-mail: johannes.fallert@physik.uni-karlsruhe.de;
Fax: +49-721-608-8480

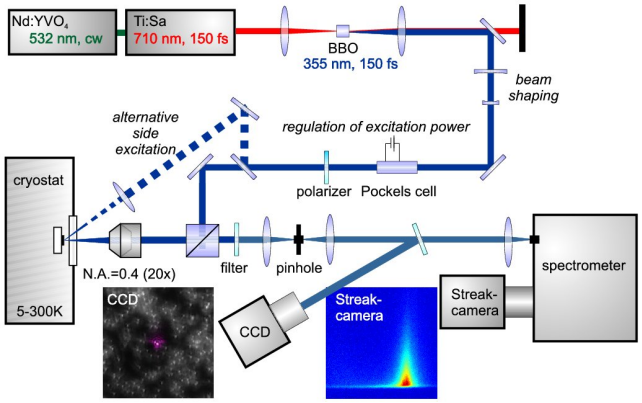

Fig. 1. Experimental setup for time-resolved micro-PL measurements of individual ZnO nanorods. The details of the setup are described in the text.

II. EXPERIMENTAL METHODS

The experimental setup is shown in Figure 1. Photoluminescence (PL) spectra are obtained using a time-resolved micro-PL system. The PL signal is recorded by using a streak-camera with a temporal resolution of 5 ps. In a He-flow cryostat, the nanorods are optically excited by using a frequency-doubled Ti:Sa laser at 355 nm (3.49 eV) with 150-fs pulse length. The excitation power is regulated by using a Pockels-cell in combination with a linear polarizer. This setup allows global excitation of an ensemble of nanorods, as well as a focusing of the excitation spot in a confocal arrangement. The spatial resolution in the latter case allows a single nanorod to be addressed. The examined nanorods are still attached as grown to the original substrate. In order to identify the measured nanorods, characteristic markers were written on the sample by using a focused ion beam (FIB). From the relative position of the nanorod to the markers, visible in the luminescence map obtained in global excitation, the examined nanorod could be retrieved with an optical microscope, as well as with a scanning electron microscope (SEM).

III. RESULTS

Above a certain threshold excitation intensity, stimulated emission is observed from the ZnO nanorods. On the one hand, the transition to the stimulated emission as the dominating radiative recombination mechanism leads to a strong increase in the PL intensity. On the other hand, the occurrence of several lasing emission lines is observed as soon as the excitation intensity is high enough to provide gain at the spectral position of the mode. The observation of laser modes is in agreement with numerical calculations of guided modes in a ZnO nanorod, which has been reported in Ref. 5. A typical

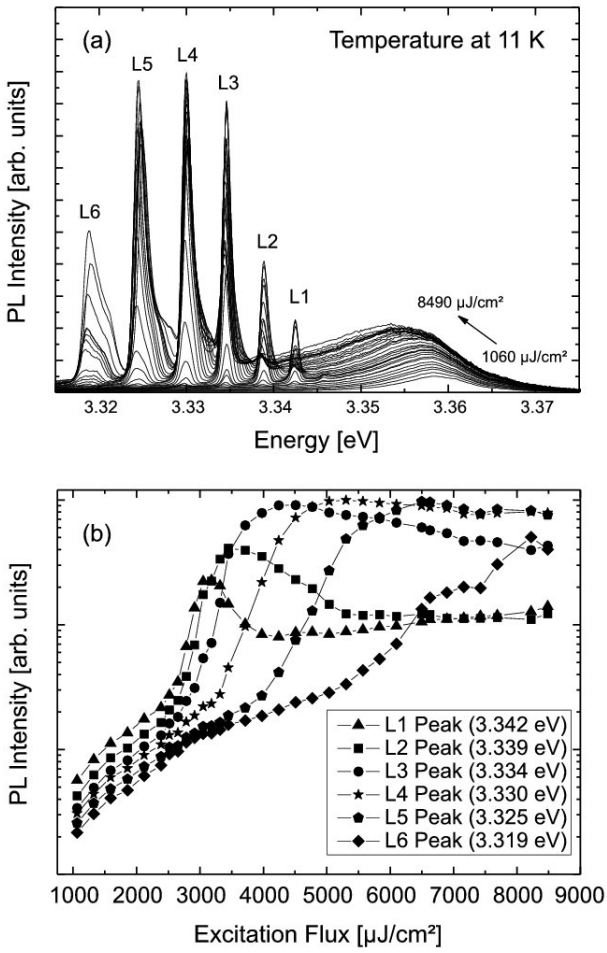

Fig. 2. (a) Under high excitation of the fs-laser, multimode lasing is observed in the ZnO nanorods. The observed laser modes are labelled from L1 to L6. (b) The peak intensities of several laser modes for varying excitation density are shown. A clear threshold behavior of each mode can be seen. Due to the gain competition among the several modes, the increasing intensity of one mode is accompanied by a decreasing intensity of another mode.

pattern of evolving modes is shown in Figure 2(a). These modes can be considered as stable features in the laser emission of the nanorod, because the spectra were taken by integrating over several millions fs-excitation pulses. The threshold behavior of the emission, as well as the gain competition among the modes, can be seen in Figure 2(b). The latter is indicated by the saturation of the emission intensity as soon as an additional mode shows stimulated emission. The main gain is provided by an inverted electron-hole plasma (EHP). In this mechanism, an increased excitation density leads to a broadening of the gain region [6], combined with its red-shift due to bandgap renormalization [7]. In a simple model, the expected gain in an EHP can be calculated by considering only direct band-to-band recombination of electron-hole pairs under momentum and energy conservation. The influence of any coulomb correlations is neglected. The

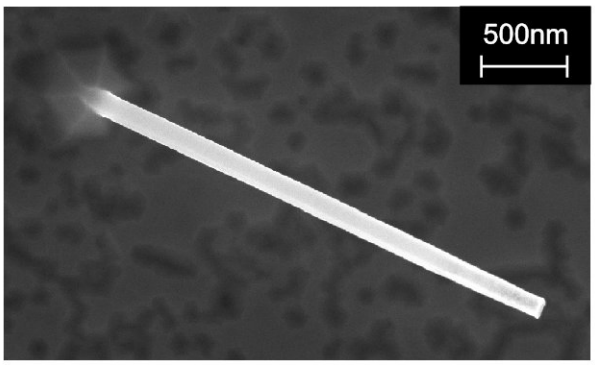

Fig. 3. A single ZnO nanorod on a silicon substrate covered with an iridium layer. The picture was taken with a scanning electron microscope. The length of the nanorod is determined from several pictures under different viewing angles as 2.9 μm and its diameter as 140 nm. By FIB-markers on the sample the position of the nanorod can be addressed and the luminescence of the particular nanorod can be measured, as shown in Figure 4.

gain, g, above the renormalized band gap energy, E_g, is then given by [8]

$$g(\hbar\omega) \propto (\hbar\omega - E_g)^{1/2}(f_e + f_h - 1) \quad (1)$$

while $g = 0$ holds for $\hbar\omega < E_g$. Here, f_e gives the occupation probability of electrons in the conduction band and f_h the occupation probability of holes in the valence band. A negative value of g corresponds to absorption. At lower excitation intensities, excitonic gain mechanisms, like the exciton-exciton scattering (the so-called P band), are also possible [9,10], but were not observed in our measurements.

Time-resolved luminescence spectra for a single ZnO nanorod with a length of 2.9 μm and a diameter of 140 nm grown on a (fcc) iridium-covered silicon substrate are displayed for various excitation intensities in Figure 4. The SEM picture of the corresponding nanorod is displayed in Figure 3. The PL was recorded in the time-resolved mode of a streak-camera. In Figure 4, only a reduced time window of 60 ps for each value of the excitation intensity is plotted to condense the data. It can be seen that above the threshold intensity, spectrally narrow lasing bands evolve, and are characterized by a rapid decay (≈8 ps decay time). This rapid decay is caused by the occurrence of lasing in the nanorod, which leads to a much higher radiative recombination rate. After this rapid decay, a relatively slow decay with a decay time of about 200 ps is observed. The same decay time is also measured at spectral positions where no laser mode appears and corresponds to the spontaneous decay of an EHP. For further increase in optical pumping, the already-mentioned gain competition leads to a saturation of modes because additional modes appear on the low-energy side of the spectra. The latter consumes a certain fraction of the available electron-hole pairs created by the short excitation pulse. At the highest pump

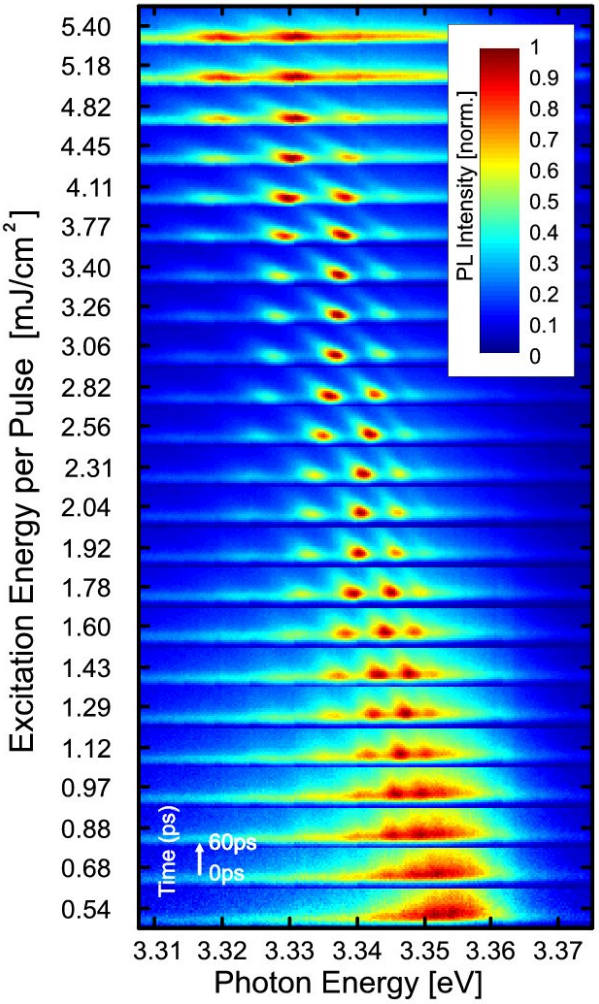

Fig. 4. The normalized spectra show the time-resolved emission at various excitation intensities of the nanorod displayed in Figure 3. In the vertical dimension, slices with a time range of 60 ps are shown. Each slice corresponds to a measurement with a certain excitation intensity. The PL intensity is encoded in the color information. Spectrally sharp and rapidly decaying spots result from stimulated emission in the modes of the nanorod.

intensities a saturation of all modes is reached and is indicated by a decrease in the emission intensity and in the line broadening. Heating of the material and possibly a starting degeneration may cause this effect.

For higher excitation power, we find a shift of the lasing modes towards higher energies. This shift can be explained by a dependency of the refractive index in the nanorod on the actual carrier density. While for low excitation densities, the refractive index in the relevant region is determined by the excitonic resonance, this resonance will vanish for increased excitation intensities and for a transition to the EHP region; hence, the refractive index will decrease. Also, in the EHP region the refractive index will still decrease with higher excitation, which can be estimated in a Drude model. Thus, the

positions of the lasing modes are shifting to higher photon energies with higher carrier densities present in the nanorod. Another shift of the lines can be found in time during their decay. This shift, in contrast, tends to lower the energies with time. The origin of this second shift can be attributed to the same physical phenomenon: the dependency of the refractive index on the carrier density. Due to radiative and non-radiative recombination, the carrier density decreases in time after the excitation pulse. With the same arguments as these above, this leads to an increased refractive index. Hence, the modes shift to the red during their decay.

The presented results are representative of the measured data for other similar nanorods on the same sample with varying spectral positions of the modes and slightly varying thresholds. Compared to the other examined ZnO nanorod samples, stronger deviations in the mode pattern occur due to the bigger difference in the nanorod geometry in terms of length and diameter. However, the described dynamics in terms of mode shift, gain competition, and bandgap renormalization is found to be the same.

IV. CONCLUSIONS

We have examined the dynamics of stimulated emission in defined single ZnO nanorods on GaN and iridium-covered silicon substrates. We show the evolution of multimode lasing in single nanorods for increased optical pumping and the gain competition among the modes. The optical gain is obviously due to an electron-hole plasma. The influence of an excitonic gain mechanism, like exciton-exciton scattering, was not observed in our measurements. Furthermore, we observed a characteristic shift of the lasing modes with time and for various excitation intensities. Both kinds of shifts are consistent with the expected behaviors of mode shifts in a resonator with a refractive index depending on the carrier density.

ACKNOWLEDGMENTS

This work was supported by the Deutsche Forschungsgemeinschaft (DFG) project KL345/23-1 and by the Landeskompetenznetz Baden-Württemberg within the Competence Network 'Functional Nanostructures', Project A1. We thank S. Gselle and M. Schreck (University Augsburg, Germany) for the preparation of the Ir/YSZ layers on silicon substrates, as well as Aixtron for providing the GaN substrates.

REFERENCES

[1] G. M. Prinz, A. Reiser, T. Röder, M. Schirra, M. Feneberg, U. Röder, R. Sauer, K. Thonke, S. Gsell, M. Schreck and B. Stritzker, Appl. Phys. Lett. **90**, 233115 (2007).

[2] R. Hauschild, H. Lange, H. Priller, C. Klingshirn, R. Kling, A. Waag, H. J. Fan, M. Zacharias and H. Kalt, Phys. Stat. Sol. (b) **243**, 853 (2006).

[3] K. van Vugt, S. Rühle and D. Vanmaekelbergh, Nano Lett. **6**, 2707 (2006).

[4] L. Wischmeier, C. Bekeny, T. Voss, S. Börner and W. Schade, Phys. Stat. Sol. (b) **243**, 919 (2006).

[5] R. Hauschild and H. Kalt, Appl. Phys. Lett. **89**, 123107 (2006).

[6] H. Priller, J. Brückner, Th. Gruber, C. Klingshirn, H. Kalt, A. Waag, H. J. Ko and T. Yao, Phys. Stat. Sol. (b) **241**, 587 (2004).

[7] P. Vashishta and R. K. Kalia, Phys. Rev. B **25**, 6492 (1982).

[8] K. Bohnert, G. Schmieder and C. Klingshirn, Phys. Stat. Sol. (b) **98**, 175 (1980).

[9] C. Klingshirn, Phys. Stat. Sol. (b) **244**, 3027 (2007).

[10] Ü. Özgür, Ya. I. Avilov, C. Liu, A. Toke, M. A. Reshchikov, D. Dogan, V. Avrutin, S. J. Cho and M. Morkoç, J. Appl. Phys. **98**, 041301 (2005).